

INF²: High-Throughput Generative Inference of Large Language Models using Near-Storage Processing

Hongsun Jang
Seoul National University
Seoul, South Korea
hongsun.jang@snu.ac.kr

Siung Noh
Seoul National University
Seoul, South Korea
siung98@snu.ac.kr

Changmin Shin
Seoul National University
Seoul, South Korea
scm8432@snu.ac.kr

Jaewon Jung
Seoul National University
Seoul, South Korea
jungjaewon@snu.ac.kr

Jaeyong Song
Seoul National University
Seoul, South Korea
jaeyong.song@snu.ac.kr

Jinho Lee
Seoul National University
Seoul, South Korea
leejinho@snu.ac.kr

Abstract

The growing memory and computational demands of large language models (LLMs) for generative inference present significant challenges for practical deployment. One promising solution to address these challenges is *offloading-based batched inference*, which leverages host memory and disk as an extended memory hierarchy for GPUs. While the approach cost-effectively enables LLM inference, its performance is limited by substantial I/O overhead, primarily due to the large key-value (KV) cache sizes, which increase with batch size and LLM context window length.

In this paper, we introduce INFERENCE-INFINITY (INF²), a framework that boosts generative inference throughput using computational storage devices (CSDs). The core of INF² is *attention-near storage*, which offloads memory-intensive self-attention operations to near-storage accelerators, significantly reducing traffic through the system interconnect. We also propose *delayed KV cache writeback* to hide storage write latency by delaying newly generated KV cache writes until the cache reaches sufficient size in system memory. Additionally, we introduce *cooperative X-cache*, a technique designed to further trade off the remaining memory capacity for storage bandwidth. Our methods effectively minimize idle time for computation, improving the overall throughput.

To demonstrate the effectiveness of our approach, INF² has been implemented on PyTorch and evaluated on a real system. Our experiments show that INF² achieves up to 3.46× throughput improvement compared to state-of-the-art baselines. We will open-source INF² to facilitate broader adoption.

1 Introduction

Transformer-based large language models (LLMs) [5, 18, 75, 93, 95, 105] are at the forefront of natural language processing (NLP), significantly influencing a wide array of user applications [1, 5, 21]. Therefore, efficiently conducting generative inference for LLMs [12, 17, 43, 51, 84] has become increasingly crucial to facilitate their use in various tasks.

One widely adopted and promising method for LLM inference is the *offloading-based batched inference* approach [54, 84], which significantly improves efficiency by processing data in numerous batches over large token sets, allowing for repeated reuse of model weights. The core idea behind this approach is to store intermediate data, specifically called *KV cache* [70], in system memory and storage devices (e.g., NVMe SSDs), extending the memory hierarchy for GPUs. Unfortunately, this approach encounters significant I/O overhead as the batch size and LLM context length increase [51, 54, 84, 106], causing the KV cache size to grow proportionally. This growth poses constraints on batch size expansion, ultimately limiting throughput. Our study reveals that KV cache I/O in offloading-based batched inference accounts for over 80% of the total inference time.

Although one might anticipate that combining multiple storage devices through a RAID solution could alleviate this issue, it is frequently hindered by the limited number of PCIe lanes on the host processor. In this circumstance, we identify that near-storage processing with computational storage devices (CSDs) can successfully address the above issue. CSDs, which have been studied for decades [4, 48, 50, 56, 82], have begun to appear as a few commercial products [86, 87, 96]. The core advantage of CSDs is their internal aggregate bandwidth exploited by the attached computational unit. By offloading appropriate computations to CSDs, we can harness their aggregated internal bandwidth, which scales linearly with the addition of more CSDs. With this advantage, we aim to address the I/O bottleneck issue of offloading-based inference with CSDs by moving KV cache-related operations to CSDs.

In this paper, we propose INFERENCE-INFINITY (INF²), a framework for high-throughput generative inference using near-storage processing devices on a real system. We introduce *attention-near storage*, which processes KV cache-related operations (specifically, multi-head self-attention) within a custom accelerator in each CSD. With attention-near storage, only the computed results are sent back to the host, significantly reducing the total I/O overhead of the KV cache.

Although near-data processing for attention operations has been explored in previous work [40, 49, 53], INF² is the first to implement a near-storage processing system on a real platform using only off-the-shelf components [31, 87], while optimizing dataflow and designing the accelerator in detail.

To realize INF² on a real system for LLM inference, one key issue is updating the KV cache stored in storage devices. Due to storage latency, involving storage write operations in the overall pipeline can severely degrade performance. To address this, we designed *delayed KV cache writeback*, which can hide storage write latency by temporally storing the newly generated KV caches in system memory until the cache reaches sufficient size. Instead of waiting for storage write completion before performing multi-head attention with the CSD, we directly forward the temporarily stored data in system memory to the CSD’s accelerator memory. The data in system memory is written to storage only when the write granularity becomes sufficiently large, ensuring efficient storage access without stalling the computation.

Additionally, considering the benefits of our CSD system, there exists room to further increase throughput by maximizing the utilization of idle resources in our system. We propose *cooperative X-cache*, a new method that reduces the total data amount to be halved through additional computations in GPU. The key idea of X-cache is storing the input activations (X) before the key-value projection layer, and at every decoding stage, we regenerate the KV cache from X in GPU. With X-cache enabled, we can take advantage of cooperative computing between the GPU and CSDs, thereby boosting overall inference throughput.

To the best of our knowledge, INF² is the first real-system implementation that utilizes CSDs to accelerate LLM inference. INF² is ready-to-use on PyTorch and implemented only with off-the-shelf hardware. Our evaluation demonstrates that INF² achieves a maximum speedup of 3.46× over the existing state-of-the-art.

Our contributions can be summarized as follows:

- We introduce attention-near storage, a system that utilizes CSDs to offload KV cache-related operations to a custom accelerator, effectively addressing the I/O overhead in offloading-based batched inference.
- We propose delayed KV cache writeback, an optimization technique that hides storage write latency when updating newly generated KV caches, improving overall performance.
- We introduce cooperative X-cache, a method that reduces the total data transfer from efficiently utilizing the host memory.
- We implement INF² on a real system, demonstrating up to 3.46× throughput improvement over the existing state-of-the-art frameworks.
- We will open-source INF² to the community.

2 Background

2.1 Transformer-based LLM Inference

KV Cache in Generative Inference. Conducting LLM generative inference is commonly categorized into two stages: the *prefill* stage and *decoding* stage. Initially, at the prefill stage, an input prompt sequence (X) is processed through the transformer model [95] and generates *key-value (KV) cache* [70], which is utilized and updated for the following decoding stages. *KV cache* refers to the key and value matrices (K, V) generated and stored in previous stages for reuse during the attention operation with the query matrix Q as follows:

$$Q = X \cdot W_Q; K = X \cdot W_K; V = X \cdot W_V \quad (1)$$

$$\text{Attention}(Q, K, V) = \text{softmax}\left(\frac{QK^T}{\sqrt{d}}\right)V \quad (2)$$

where W_Q, W_K, W_V matrices are weight projection matrices. d denotes the hidden dimension of multi-head attention (MHA). In the following MLP, the output matrix is once projected by a linear layer (W_O) and then applies two additional linear transformations (W_{MLP}) with *GeLU* or *SiLU* [30, 39, 85]. After the prefill stage, the decoding stage iteratively generates the next single token by performing the attention operation and reusing the KV cache. The newly generated KV caches for each iteration are appended with the previously generated KV caches. At every decoding stage, the KV cache from previous stages is recurrently reused and this can significantly improve the overall LLM inference throughput [54, 70, 84].

2.2 Offloading-based Batched Inference

As described in Section 1, the substantial memory requirements for LLM inference necessitate using dozens of GPUs to keep the entire data in the memory, significantly increasing the system costs. A popular low-cost alternative is to utilize system memory and storage as an extension to the GPU memory, a technique known as *offloading-based batched inference*. Figure 1 illustrates the procedure of offloading-based batched inference [12, 84] for a single layer, utilizing secondary storage as an extended GPU memory hierarchy. For simplicity, we assume that at least one layer fits within the GPU memory, and the model states in half-precision fit within system memory, with ‘Host’ referring to both the CPU and GPU.

Prefill Procedure. In the prefill stage (Figure 1(a)), ① the GPU initially loads the attention layer weights and the output of the previous layer as input. ② Once the weights are loaded, the inputs are multiplied with them to generate query, key, and value matrices. ③ These matrices are used to calculate attention scores for the input prompt sequence via multi-head attention. ④ Next, the MLP layer weights are loaded from system memory, ⑤ and the final output activations of the transformer block are generated. ⑥ The generated KV cache is written back to system memory (to storage

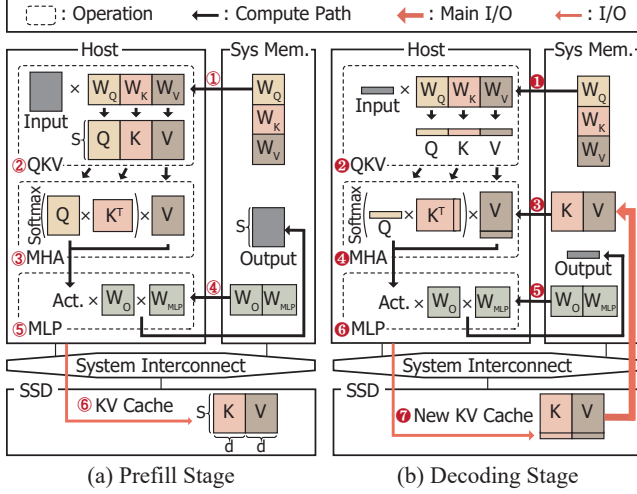


Figure 1. Overall procedure of offloading-based batched inference [12, 84]. (a) At the prefill stage, the KV cache is generated for input prompt sequence and stored in the storage. (b) At the decoding stage, each MHA layer loads the stored KV cache from storage to compute attention scores.

if memory capacity is exceeded). Steps ① through ⑥ are repeated for each transformer block, ensuring overlapping data transfers and computations. The outputs of the prefill stage are the KV cache for the input prompt sequence and the prediction of the first output token.

Decoding Procedure. The following decoding phase, illustrated in Figure 1(b), proceeds as follows: First, ① the GPU retrieves the weights of an attention layer and the output of the previous layer as input. ② The GPU then performs the QKV projection. ③ Unlike in the prefill stage, the stored KV cache for each layer is loaded for multi-head attention (MHA) computation. ④ Note that the MHA computation is performed on the CPU using the loaded KV cache. Since MHA primarily involves less computationally intensive General Matrix-Vector Multiplication (GEMV) operations, it can be efficiently handled by the CPU, avoiding the need to transfer the KV cache to the GPU via PCIe interconnect for computation [54, 84]. ⑤ The generated output activations are transferred back to the GPU from CPU, and the weights (W_O , W_{MLP}) for the MLP computation are loaded onto the GPU. Then, ⑥ the GPU processes the MLP computation. Finally, ⑦ the newly generated KV cache for the newly generated token is written back to the original location of the KV cache for future decoding stages. This decoding process (① through ⑦) is repeated iteratively for each transformer block, with the entire inference process for all layers continuing until the model generates an end-of-sequence token or the number of generated tokens reaches the requested output length.

I/O Analysis. With offloading-based batched inference, there is a significant benefit from reducing the total number of weight loads for computation, which scales with the batch

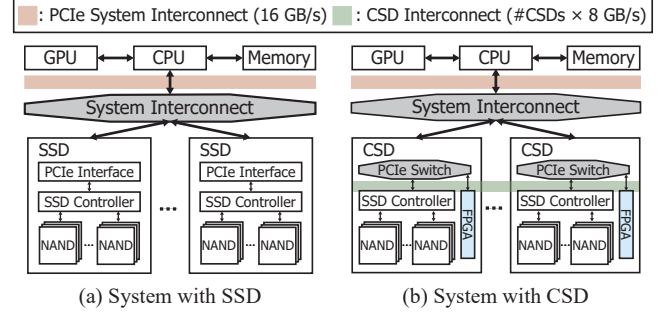


Figure 2. (a) An example of PCIe hierarchy with standard storage devices (b) An example of an environment with computational storage devices (e.g. SmartSSD [87]).

size and leads to high throughput. However, this method incurs considerable I/O overhead due to the large size of the KV cache. To quantify the total traffic, let the batch size be represented by b , the input sequence length by s , the output sequence length by n , the number of attention heads by h , and the hidden dimension per head by d . The prefill stage can be considered at iteration $i = 0$, while subsequent stages in the range $[1, n]$ correspond to the decoding stages.

During the prefill stage, the total KV cache write size in bytes per transformer block is $s \cdot 2 \cdot (K \text{ and } V) \cdot b \cdot h \cdot d \cdot 2$ (FP16). In the decoding stage, the read traffic in bytes per transformer block for attention operations is $(s + i - 1) \cdot 2 \cdot (K \text{ and } V) \cdot b \cdot h \cdot d \cdot 2$ (FP16). The write traffic in bytes per transformer block, for updating the KV cache, is $2 \cdot (K \text{ and } V) \cdot b \cdot h \cdot d \cdot 2$ (FP16). These data transfers pass through the system interconnect (PCIe), as illustrated by the red arrows in Figure 1. Our work, INF², aims to minimize such data transfer over the system interconnect by placing accelerators within CSDs, while addressing key system integration challenges for high throughput LLM inference.

2.3 Computational Storage Devices

Computational storage devices (CSDs) [4, 48, 55, 103], or near-storage processing [4, 82, 83, 103], have been explored extensively over the decades. By placing a computational unit close to storage devices, workloads can benefit from reduced latency, decreased bandwidth consumption, and less computational pressure on the host. Various types of CSDs that recently started to appear on the market [86, 87, 96] share two common features. First, a light-weight accelerator is placed near storage. Second, there exists a private inner path between the storage device and the attached accelerator.

Figure 2(a) depicts an example of PCIe topology with common storage devices. In contrast, Figure 2(b) illustrates an environment featuring CSDs, which introduces a key distinction: an internal PCIe switch between the storage device and the attached accelerator, which provides a private pathway for direct peer-to-peer (P2P) communication [16, 104]

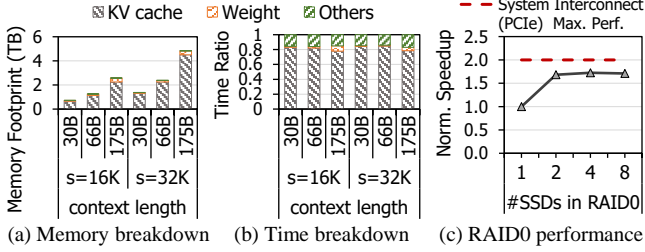


Figure 3. A motivational study. s represents the LLM input context size, and B denotes the model parameter count. (a) Memory consumption breakdown during offloading-based batched inference. (b) The main bottleneck in offloading-based LLM inference is KV cache traffic. (c) Scaling storage devices with RAID0 fails to improve performance due to the bandwidth limits of the shared PCIe interconnect.

between the NVMe device and the accelerator, eliminating redundant data traffic to and from the host over the system interconnect [44, 80, 81]. A single CSD does not inherently increase bandwidth, as both SSD-to-FPGA and SSD-to-host transfers occur over sufficient PCIe lanes. However, when multiple CSDs are deployed, the combined internal bandwidth scales linearly with the number of CSDs, while the bandwidth of the shared system interconnect remains constant. Nonetheless, adding multiple CSDs does not automatically result in speedup. Achieving high performance requires careful consideration of several key factors: (1) determining what computations should be offloaded to the CSD (Section 4.1), (2) effectively hiding storage write latency (Section 4.2), and (3) effectively scheduling the CSD with the host (Section 4.3).

3 Motivational Study

In this section, we analyze the main bottleneck of offloading-based batched inference through a motivational study and examine the existing challenges. For details on the experimental setup, please refer to Section 7.1. Figure 3(a) presents the breakdown of the required data for conducting offloading-based batched inference, where we categorized memory consumption into three parts: KV cache, LLM weight, and others (e.g., activations). Notably, the KV cache for long-context-length LLMs requires terabyte-scale memory, making the use of storage devices necessary in resource-limited scenarios. As a result, as shown in Figure 3(b), which provides the breakdown of time with a state-of-the-art baseline [84]. More than 80% of the total time is spent on KV cache-related I/O when storage is used. This data transfer overhead increases significantly with larger models and longer context lengths [15, 46, 59, 102], making it a critical challenge in offloading-based batched inference.

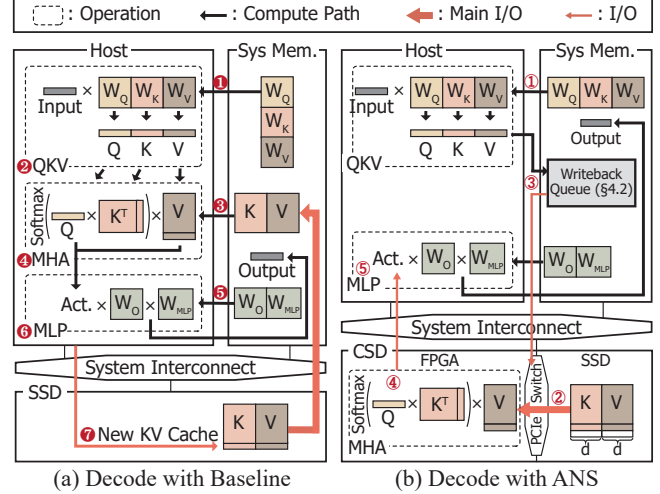


Figure 4. The overall procedure of the decoding stage for (a) the baseline and (b) Attention-near storage. In the baseline, the KV cache is loaded from storage to the host through the system interconnect. With Attention-near storage, the KV cache is loaded from storage directly to our custom accelerator via an internal PCIe switch.

One straightforward approach to alleviating the data transfer overhead of storage devices is to increase storage bandwidth using a RAID solution. Figure 3(c) demonstrates the normalized speedup of offloading-based batched inference when scaling the number of storage devices using RAID0. Unfortunately, the offloading-based batched inference with RAID0 experiences a bottleneck due to the traffic of the KV cache on the shared system interconnect, which becomes a bottleneck when using more than three SSDs. Moreover, KV cache-related I/Os are predominantly read operations, which generally provide higher bandwidth than write operations in modern storage devices. Thus, utilizing the RAID solution for offloading-based batched inference has its limitations.

The motivational study above shows that the data transfer overhead issue of the KV cache cannot be easily addressed due to the limited shared system interconnects of the existing system structure. On the other hand, properly using CSDs can mitigate the bottleneck as they can provide more internal bandwidth than the system interconnects. Our primary objective is to minimize the data transfer between storage devices and host memory by leveraging the aggregated bandwidth from the direct path inside each CSD.

4 INFERENCE-INFINITY (INF²)

4.1 ANS: Attention-Near Storage using CSD

As discussed in Section 3, the volume of KV cache communication during the decoding stage is substantial in the offloading-based batched inference. With traditional storage devices, this communication must traverse the shared system

interconnect to perform attention operations on the CPU. To mitigate this bottleneck, we propose *attention-near storage* (ANS), a novel system that shifts attention computation to a custom accelerator within computational storage devices (CSDs). This approach enables KV cache read traffic to leverage the fast aggregated bandwidth of CSDs, while only the input and output of the multi-head attention pass through the system interconnect.

At the prefill stage, the initially generated KV cache is written to the storage device within the CSDs as in the baseline (Figure 1(a)). The proposed ANS differs from the baseline (Figure 4(a)) in the decoding stage, as illustrated in Figure 4(b).

① The required attention layer weights and input activations are loaded into the GPU from system memory, similar to the baseline. ② The necessary KV cache is directly loaded from each storage device to the attached accelerator via direct P2P communication through the private PCIe switch within each CSD. ③ The host generates the query, key, and value vectors from the QKV projection and loads them into the memory of each accelerator within the CSDs. ④ Once the accelerator completes the multi-head attention (MHA) computation, the output vectors are transferred back to the host. ⑤ The GPU then proceeds with the MLP computation.

By computing the MHA layer close to the storage using attention-near storage, each accelerator can directly access the KV cache via the private path within the CSD, significantly reducing read data traffic through the system interconnect. When quantifying the data traffic at the first iteration of the decoding stage, attention-near storage significantly reduces the read traffic through the system interconnect from $s \cdot 2 \cdot (K \text{ and } V) \cdot b \cdot h \cdot d \cdot 2$ bytes in the baseline for reading the KV cache to $b \cdot h \cdot d \cdot 2$ bytes for reading the new attention score. The write traffic through the system interconnect slightly increases from $2 \cdot (K \text{ and } V) \cdot b \cdot h \cdot d \cdot 2$ bytes for writing the new KV entry to $3 \cdot (Q, K, \text{ and } V) \cdot b \cdot h \cdot d \cdot 2$ bytes for sending the new Q, K, and V entry. Overall, the total traffic is significantly reduced. This is because most of the KV cache read traffic is handled via the internal bandwidth of the CSDs, with only the output vectors from the accelerator being transferred through the system interconnect.

When ANS is implemented with a single CSD, the bottleneck simply shifts from the system interconnect to the CSD’s internal switch. However, the true benefit becomes evident as the number of CSDs increases. As more CSDs are added, the aggregate bandwidth between the FPGA and SSD scales linearly, while the bandwidth to the host via the system interconnect (PCIe) remains constant. While there is a minor benefit from the increased computational capacity of more FPGAs, the main driver of the speedup in INF² comes from leveraging the aggregated internal bandwidth.

We can quantify that attention-near storage reduces the data traffic through the system interconnect by a factor proportional to the sequence length s when assuming a sufficient

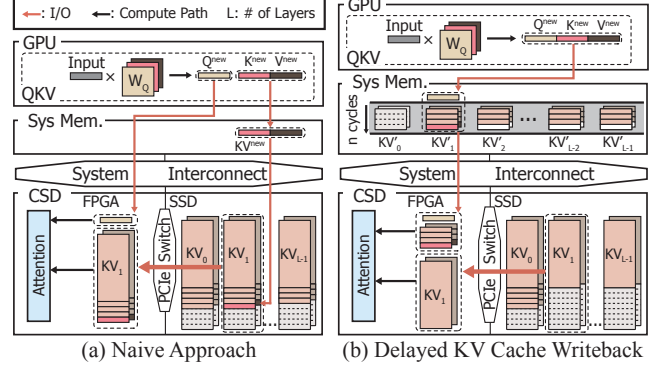


Figure 5. KV cache writeback procedure. (a) Naive decode stage with attention-near storage. (b) Decode stage with delayed KV cache writeback.

number of CSDs. Let T_{BASE} be the traffic with the baseline and T_{ANS} be the traffic with attention-near storage.

$$\frac{T_{BASE}}{T_{ANS}} = \frac{4sbhd + 4bhd}{2bhd + 6bhd} = \frac{s + 1}{2} > 1 (\because s > 1). \quad (3)$$

To utilize multiple CSDs, we parallelize along both the batch dimension and the head dimension in MHA. In offloading-based batched inference scenarios, batch sizes are typically large to minimize LLM weight transfer overhead. Since the total available parallelism is the product of the batch size and the number of attention heads, there are sufficient dimensions to effectively distribute the workload across the CSDs. As a result, during the decoding stages, MHA computation is performed entirely through intra-CSD communication between the attached FPGA and SSD, eliminating the need for inter-CSD communication. To enable this, we distribute the KV cache generated in the prefill stage across the CSDs using these parallel dimensions. The KV cache is initially stored in an $s \times d$ array format, with pre-allocated space for the newly generated KV cache based on the provided maximum sequence length (n). This allows the newly generated KV cache to be appended to the existing cache sequentially in d -byte chunks.

4.2 Delayed KV Cache Writeback

One critical challenge from attention-near storage is that the newly generated key and value vectors from each decoding iteration must be written back into the KV cache within each storage device. Because the FPGA has to reread it for the MHA, the long latency quickly becomes the system bottleneck. Furthermore, parallelizing along the head dimension yields small write granularity, which is inefficient for SSDs.

To address this issue, we propose *delayed KV cache writeback*. In the naive way with ANS in Figure 5(a), a new KV entry is first written to the KV cache in the SSD. Then, the grown KV cache is transferred to the in-CSD FPGA for the attention operation. In this method, the SSD write is on the

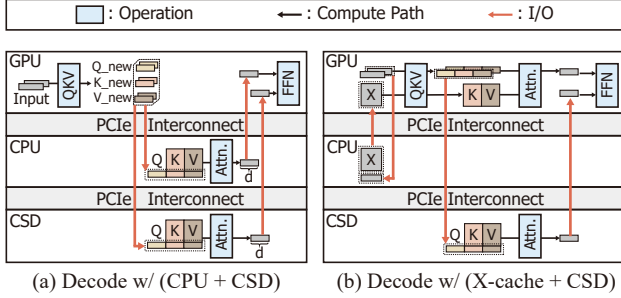


Figure 6. Cooperative computing procedure with (a) KV-cache and (b) X-cache.

critical path. Furthermore, a single KV entry is far smaller than the SSD page size, harming the write performance.

With delayed KV cache writeback shown in Figure 5(b), instead of writing each newly generated KV cache entry directly to the storage device, We maintain dedicated buffers for the KV caches in the host memory, and let the buffer directly feed the FPGAs in the CSD. The existing KV cache is provided by the SSD. This optimization takes SSD write latency off the critical path. After the predefined interval of c decoding iterations, they are spilled to the storage device in bulk, off the critical path.

Through delayed KV cache writeback, we achieve several benefits: 1) storage write latency is effectively hidden, and 2) the total data written to storage is handled in larger chunks, improving the efficiency of the storage device. A small downside is that the same KV cache values are redundantly sent through the system interconnect from host memory to the FPGAs until they are spilled. However, we found the benefits to be much larger than the small drawbacks in practice.

4.3 Cooperative X-cache Optimization

Applying ANS and delayed KV cache writeback ensures the CPU memory footprint remains constant, leaving additional room for cooperative computing between the host and CSDs. One straightforward method is to store a portion of the KV cache in the host memory and let the CPU perform MHA, as shown in Figure 6(a). This significantly reduces the traffic through the system interconnect.

To achieve even higher performance, we further propose cooperative X-cache as shown in Figure 6(b). According to Equation (1), the KV cache is calculated by $K = X \cdot W_K$ and $V = X \cdot W_V$. From this, we choose to cache X in the host memory instead of KV, which we denote as X-cache. Because X-cache occupies only half the memory compared to KV cache, this has the effect of reducing the system interconnect traffic twice more than the CPU performing MHA with the same memory budget. The additional overhead is in regenerating K and V which involves recomputing the QKV projection on the GPU. However, we find that this overhead is almost negligible compared to the reduced data. Compared to the

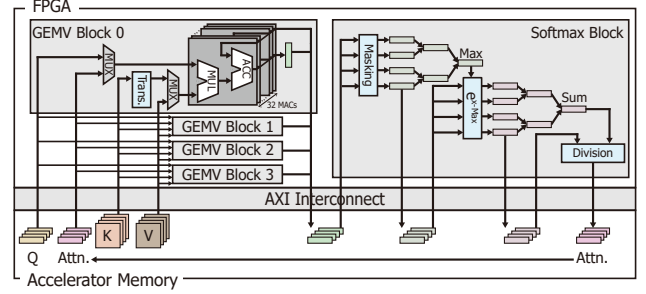


Figure 7. Microarchitecture of custom accelerator for KV cache-related operations.

KV cache-based cooperation, X-cache also slightly benefits from letting the CPU focus on I/O management [19, 74, 97] to draw maximum bandwidth.

While our approach is straightforward, it yields performance improvements by significantly reducing the size of intermediate data and minimizing idle time for computing components. Contrary to existing offloading systems, X-cache gains more performance as more memory is added to the system, which is quantified in Section 7.5.

5 Accelerator Microarchitecture

Figure 7 illustrates the hardware accelerator architecture implemented in the FPGA of the CSD to support INF². For multi-head attention [95] implementation, the accelerator consists of two primary modules: *GEMV* and *softmax*. The *GEMV* module handles the necessary linear transformations and optionally transposition, while the *softmax* module normalizes the attention scores, enabling the correct weighting of different input features.

The GEMV blocks are used for multiplying Q with K^T and then multiplying the softmax results with V . For this, each GEMV block comprises 32 MAC units to perform inner products. Because we need to multiply K^T , we provide an optional transpose module to perform the necessary transpose for the key matrix (K). An alternative would be storing K in a transposed format in the SSD, but the number of rows of K continuously grows each iteration, and storing this in a transposed format makes the growth very difficult to manage. To support the transpose without extra read/write to the accelerator DRAM, we load 32×32 FP16 values to the FPGA BRAMs and perform in-place transposition. Then the MAC units perform blocked GEMV, multiplying a 32-element vector to a 32×32 matrix and accumulating results to the output activation buffer. From this, the same GEMV block can be reused for the two GEMV operations (for K^T and V) with a few multiplexers. This optimization significantly reduces resource utilization for our accelerator, which is crucial for the lightweight FPGAs in CSDs. Once the results are computed across the four GEMV blocks, they are stored back into the accelerator memory for further processing.

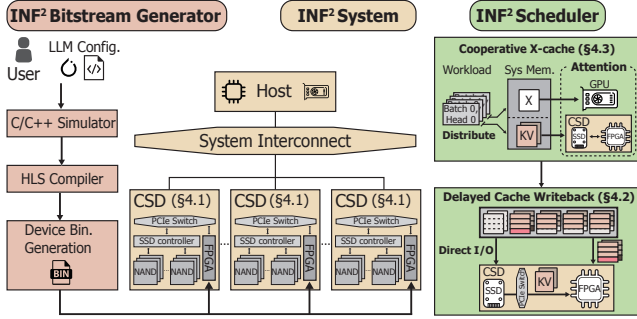


Figure 8. Overview of INF^2 , which is a ready-to-use framework. Users can perform their own LLM model’s inference procedures with INF^2 system.

The softmax module operates in three main steps: (1) masking while finding the maximum value, (2) computing the exponential sum, and (3) performing division. This multi-step approach is necessary due to the inherent reduction dependency in the softmax operation [24, 25, 61, 62]. First, the masking module loads 128 data elements into four buffers each cycle and overwrites the masked values to a negative constant $-1e4$ based on masking information received from the host (e.g., padding or current decoding stage iteration). To find the maximum value, which scales the exponential for numerical stability, a hierarchical reduction approach is used. Four parallel units compute the maximum value within each group of 32 elements. Once all elements have been processed, the four intermediate maximum values are reduced to a final maximum using a two-step tree structure. Second, the module then computes the exponential values from the masked data (32×4). The sum reduction follows the same hierarchical reduction approach used in the previous step. FP16 is used for accumulation, ensuring numerical stability while offering sufficient precision. Finally, the module reads the stored exponential values and divides each by the sum value from the previous step. The results are then stored back in accelerator memory for the next GEMV operation.

6 Implementation

Bitstream Generator. The procedure to generate bitstream is described on the left side of Figure 8. The pre-compiled device binary codes are sufficient to execute INF^2 without any synthesis. If customization is needed, our synthesizable device codes can be customized via modifying high-level synthesis (HLS) codes [11, 66]. Customizing the accelerator can be challenging, even with the synthesizable HLS template and helper tools [36, 37]. To ease the difficulties, we provide a C/C++-based simulator integrated into the LLM codes in PyTorch to check the functionality of the accelerator.

INF^2 System. INF^2 system is described in the middle side of Figure 8. The INF^2 system consists of attention-near storage (Section 4.1) and our custom accelerator (Section 5, Section 7.2), utilizing a general PCIe expansion system [31, 44, 74, 90] to equip multiple CSDs with limited PCIe lanes in the host. While this solution does not increase the raw link bandwidth to the host, INF^2 leverages the internal bandwidth of CSDs to mitigate the high I/O demands. To enable direct P2P communication [16, 104] between the NVMe SSD and FPGA, we allocate a special Xilinx OpenCL extension buffer [3] in the device memory, which facilitates interaction with the attached storage device at runtime. When writing data to the storage device, it is crucial to identify which FPGA is directly connected to the specific SSD via its internal PCIe switch. To simplify this process, INF^2 includes automatic identification of the PCIe topology, matching each SSD with its corresponding FPGA. Once matched, standard Linux system calls (`pread/pwrite`) can be used for direct P2P data transfer between the SSD and FPGA.

INF^2 Scheduler. The host program consists of a scheduler responsible for managing the operations of delayed KV cache writeback (Section 4.2) and X-cache (Section 4.3). The scheduler is implemented in C++ and communicates directly with the PyTorch application using `pybind11` [72]. Our module is provided as a callable function, utilizing `distutils` [28] to build C/C++ implementations as additional Python modules, with automatic compilation initiated when the engine starts.

The detailed procedure of the scheduler is described in the right side of Figure 8. First, the scheduler estimates the memory footprint required for performing offloading-based batched inference and allocates portions to CSDs and for X-cache accordingly. Second, following the workload distribution, the scheduler executes the prefill stage, storing the KV cache in the appropriate locations. Third, during the decoding stage, execution occurs in parallel according to the workload distribution. When delayed writeback buffers (Section 4.2) reach the designated threshold, the scheduler initiates a write operation to the SSDs independently from the LLM inference pipeline. To ensure data is correctly stored, direct I/O must be used for CSD applications. Because the newly generated KV cache entries are smaller (sized at 256B [75, 93, 94, 105]) than the minimum write granularity for direct I/O (512B), using a spill interval c larger than 1 for delayed KV cache writeback is recommended.

7 Evaluation

7.1 Experimental Setup

Our experimental setup is detailed in Table 1. We implemented and evaluated INF^2 on a system equipped with 16 Samsung SmartSSDs [87], connected to the host via a PCIe expansion [31] to increase the system’s physical slots. Each SmartSSD includes a 4TB NVMe SSD and a Kintex Ultra-Scale+ KU15P FPGA with 522K LUTs, 984 BRAMs, 128 URAMs,

Table 1. Experimental Environment.

HW	GPU	NVIDIA A100 (40GB), H100 (80GB)
	CPU	Xeon(R) Gold 6342, 2×48C 96T
	Memory	32×32GB DDR4-3200
	CSD	SAMSUNG SmartSSD [87], 4TB
	PCIe Expansion	H3 Falcon 4109
SW	OS / Python	Ubuntu 20.04 LTS / 3.12.4
	PyTorch / DeepSpeed	2.4.1 / 1.15.1
	Vitis / XRT	2023.1 / 2.12.427
	CUDA / OpenCL	12.1.105 / 2.2

Table 2. Resource Utilization of Implementation for ANS.

LUT (522K)	FF (1020K)	BRAM (984)	URAM (128)	DSP (1968)
47.36%	32.72%	47.10%	9.38%	13.26%

1968 DSPs, and 4GB of DDR4-2400 DRAM. The SSD can directly communicate with the attached FPGA through a PCIe 3.0×4 lanes. Our setup also includes either an NVIDIA A100 or H100 GPU, both widely used for LLM inference, connected to the CPU via PCIe 4.0×16 lanes.

For the existing baselines described in Section 2.2, we used FlexGen [84] (**FLEX**) as the state-of-the-art framework for offloading-based batched inference. Additionally, we evaluated DeepSpeed [41] (**DS**) with the ZeRO-Inference [12] option enabled, which supports KV cache offloading to main memory and weight offloading to storage. Since DeepSpeed does not support KV cache offloading to storage, we used swap memory for evaluation. For both FlexGen and DeepSpeed, we enabled the option to perform attention computation on the CPU. We also considered Accelerate [43] (**HF**) as a baseline. All baselines were set up with software RAID0 using Linux mdadm [2], and for a fair comparison, we used the NVMe SSD of the SmartSSD in all tests.

For our work (**INF2**), we prioritized parallelization along the batch dimension, and then the attention heads. The default storage spill interval c , for the delayed writeback buffers, was set to two. We evaluated two representative decoder-only models, OPT [105] and LLaMA-2 [94], in FP16. We used a default batch size of 32, as our goal was to improve the throughput of offloading-based batched inference. Only when the model weights could not fit into GPU memory, they were stored in main memory, and the default output sequence length was set to 64. To measure the effect of different system memory budgets, we used the `systemd` command to adjust memory allocation, with 512GB as the default.

7.2 Implementation Results

Our accelerator, described in Section 5, is implemented on a real system using off-the-shelf components, as shown in

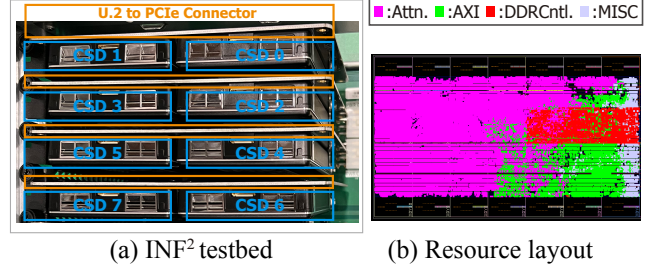


Figure 9. (a) Proposed system for INF². (b) Resource layout of the implemented accelerator (Section 5) on SAMSUNG SmartSSD [87]. Only the user logic partition (ULP) is shown, excluding the base logic partition (BLP) region, which is typically provided by the vendor.

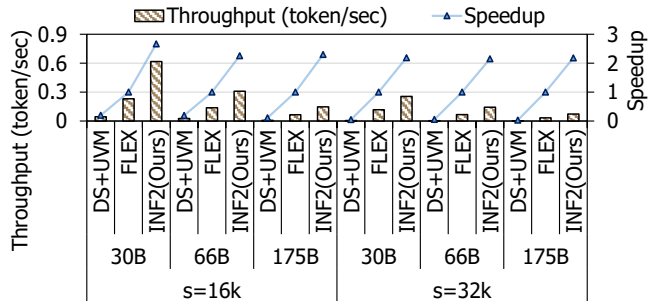


Figure 10. Throughput and speedup of our approach (INF²) compared to baselines, using an A100 GPU. DS+UVM represents the results with DeepSpeed [41] with UVM [9] enabled, while FLEX refers to the results of FlexGen [84].

Figure 9(a). The setup includes 8× PCIe 4.0 x8 lanes, with each x8 lane connecting two CSDs via 2×U.2 to PCIe connector. Each CSD operates at PCIe 3.0 x4 lanes speeds, as the connection speed is matched to the lower generation.

Figure 9(b) illustrates the final resource layout of our accelerator implemented on the FPGA of the SmartSSD [87]. In the layout, the attention logic consumes a significant portion of the area, particularly the softmax logic, which involves computationally expensive exponential operations using DSPs. Table 2 details the resource utilization of our accelerator implementation on the FPGA. Note that there is still available logic on the lightweight FPGA [10], which may allow for additional operations to support other variations [7]. The total on-chip power consumption is 14.21W. Thus, even with 16 CSDs utilized (227.36W), the power consumption is comparable to that of a single GPU, which typically requires several hundreds of Watts.

7.3 Performance Comparison

We measured the throughput of both baselines (FLEX, DS) and INF² in Figure 10, using an A100 GPU with model sizes from 30B to 175B parameters. Due to GPU OOM issues in

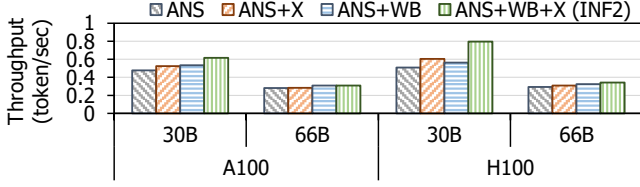


Figure 11. Ablation study of INF² using 16 CSDs with batch size of 32 and 16K cont. ANS indicates attention-near storage, ANS+X means ANS with X-cache enabled, ANS+WB refers to ANS with delayed KV cache writeback enabled, and ANS+WB+X indicates applying all the proposed methods.

DS with long context lengths during the prefill stage, we enabled unified virtual memory (UVM) [9] for measurement. Both INF² equipped with 16×CSDs and the baseline were tested with the same number of storage devices.

DS suffered more than 5× throughput loss compared to FlexGen due to UVM overhead, so the speedup was normalized to FlexGen results. INF² consistently showed more than 2× speedup across all setups, with 2.67× for 30B model and 2.3× for 175B model with 16K LLM context length. The slightly less speedup for the 175B model is due to its larger memory footprint of model weights stored in the main memory (over 300GB), leaving less room for X-cache.

7.4 Ablation Study Results

Using the setup only with our first technique (attention-near storage) as the baseline (ANS), we evaluated the throughput improvement when the proposed schemes were applied, as shown in Figure 11. When X-cache is enabled (ANS+X), we observed a 1.07× to 1.19× speedup compared to ANS alone. The speedup is more significant with the H100 and the 30B model, as X-cache benefits from the performance of GPU and the larger available main memory. When delayed KV cache writeback is enabled (ANS+WB), we observed a 1.10× to 1.12× speedup over ANS, highlighting the importance of hiding storage write latency in CSD applications. When all proposed techniques are applied (ANS+WB+X), the speedup ranges from 1.1× to 1.57× compared to ANS alone.

7.5 Sensitivity Test Results

Batch Size and Model Residency Ratio. Both the state-of-the-art baseline and INF² support model weight offloading to SSD, which helps reduce the main memory burden for storing model weights. In Figure 12, 100% indicates that the model weights are fully stored on the SSD, while 0% means the weights are entirely held in main memory. As expected, when the batch size is 1, the KV cache can fit into main memory, resulting in no storage traffic for both the baseline and INF². However, with a batch size of 1, there is a significant throughput loss due to the overhead of loading weights, especially when the model weights are fully stored on the

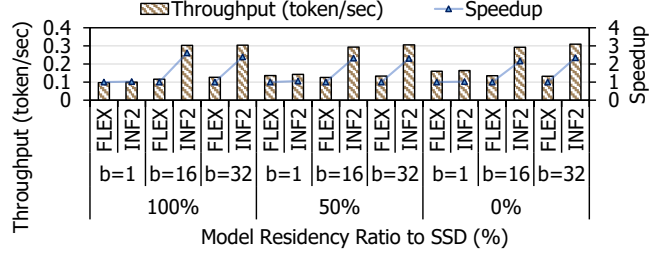


Figure 12. Sensitivity study to batch size (b) and model residency ratio to SSD (%) using 66B model with a 16K context length on an A100 GPU. 100% indicates that the model weights are entirely stored on the SSD, while 0% indicates that the weights are fully held in main memory.

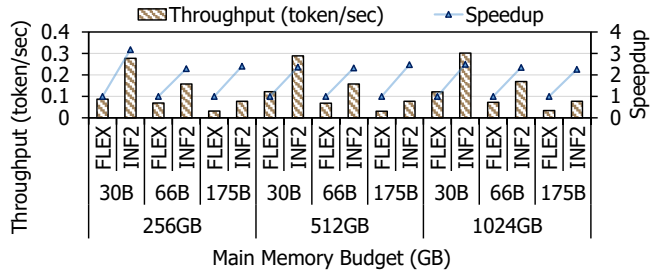


Figure 13. Sensitivity study to different main memory budgets. H100 GPU and a 32K context length are used.

SSDs (100%). When the batch size is increased, FlexGen only succeeds in increasing throughput for the results of 100%, but fails to improve throughput in the other two cases (0%, 50%). In contrast, INF² successfully improves throughput across all setups. Interestingly, as the weight ratio in SSD increases, throughput of INF² also improves. This is because offloading model weights to SSD frees up main memory, allowing X-cache to be applied to a larger portion of the workload. This ability to achieve higher throughput while storing weights on SSD is a significant advantage, especially as model sizes grow, making INF² highly scalable for larger models.

Memory Budget. INF² benefits from fully utilizing main memory space through X-cache, making it valuable to discuss the results based on different memory budgets. In Figure 13, although the throughput of the baseline [84] improves with more main memory, INF² consistently achieves a 2.26×-3.18× speedup across various memory budgets ranging from 256GB to 1TB. This is because X-cache allows INF² to fully utilize the increased main memory space. For larger models, the improvement with the baseline, ranging from 256GB (0.032 token/sec) to 1TB (0.034 token/sec), indicates that simply increasing main memory may not be the ultimate solution when KV caches exceed the CPU memory budget significantly. In contrast, INF² achieves a 2.26× speedup over the baseline with 175B model.

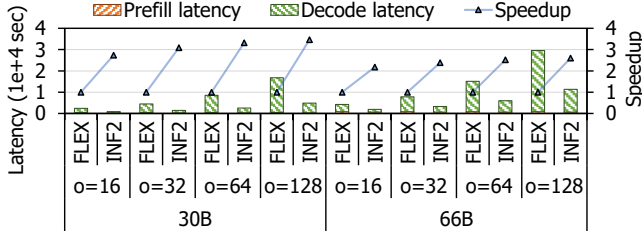


Figure 14. Breakdown of total execution time based on output length (o) and model size (B). For this experiment, a 16K context length and an H100 GPU were utilized.

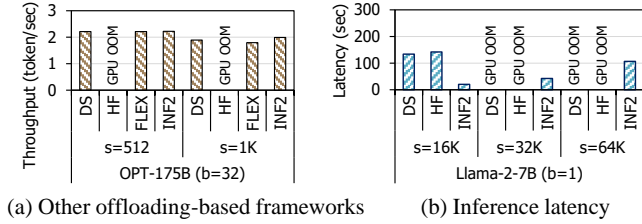


Figure 15. Performance analysis (a) with shorter context length (s) comparing existing frameworks (DS refers to DeepSpeed with ZeRO-Inference [12] enabled, HF refers to Hugging Face Accelerate [43]) and (b) model sensitivity on Llama-2 [94] with long context lengths.

Output Sequence Length. Figure 14 shows the performance sensitivity to output length (o) and model size (B). As described in Section 4.1, we preallocate space in storage at prefill stage for the newly generated KV cache based on the maximum output length, making it important to assess performance sensitivity to varying output lengths. The results indicate that increasing the length of the generated sequence rather improves the speedup compared to the baseline, with speedups of up to 3.46 \times . This is because the prefill stage latency remains constant, while the proportion of time spent on the decoding stage increases. This effectively compensates for any additional traffic from preallocated storage space. As a result, INF² consistently provides performance improvements regardless of the generated sequence length, making it particularly well-suited for generating long outputs.

7.6 Comparison with General Frameworks

In Figure 15, we provide comparisons with additional baselines of DeepSpeed [12, 41] without UVM (DS) and Accelerate [43]. Because they faced OOM issues for our main performance comparison, we conducted experiments using far shorter context lengths and smaller models. The experiments were conducted using an H100 GPU with a 1TB main memory budget. Accelerate (HF) fails to support the 175B model, while other baselines like DeepSpeed (DS) and FlexGen are able to provide support with performance comparable to our approach. This outcome is expected, because the KV cache

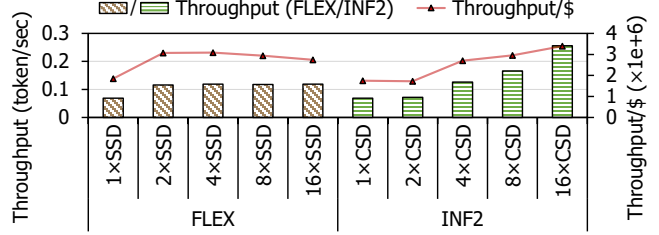


Figure 16. Cost-effectiveness comparison with scaling the number of SSDs. The experiments are conducted with 30B model with an H100 GPU and a 32k context length.

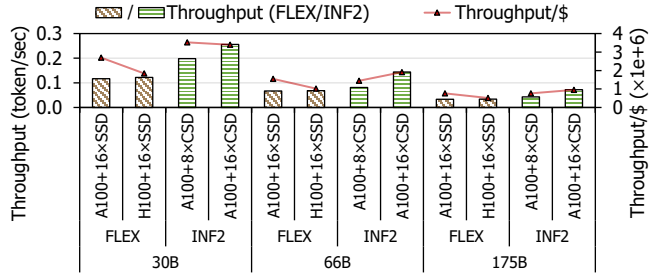


Figure 17. Cost-effectiveness comparison with higher-grade GPUs.

size is relatively small (less than 100GB) for short sequences, which fits entirely into system memory. As a result, no storage traffic is required, and thus no significant speedup can be observed under these conditions. Both DeepSpeed and Accelerate also support a variety of models. Thus, we also evaluated INF² with LLaMA-2 [94] in Figure 15(b). However, both baselines struggle with long context lengths beyond 16K, even for relatively small models like 7B, and even with a batch size of 1. This issue is caused by GPU OOM errors during the prefill stage. This highlights a key limitation in current frameworks for supporting long context lengths, aligning with findings from recent works [61, 62].

7.7 Cost-Effectiveness Comparison

Against adding SSDs. We first compare the cost-efficiency of adding more storage devices. In Figure 16, experiments with a 30B model, H100 GPU, and 32k context length were conducted. Our experimental setup costs \$37,000 (A100: \$7,000, server: \$20,000, expansion: \$10,000), with each SSD costing \$400 and each CSD costing \$2,400. Initially, the baseline [84] with 2 \times SSDs outperforms INF² in cost-efficiency, achieving a 1.68 \times speedup compared to the single-device setup. This is expected, as two SSDs do not saturate the system interconnect. However, the baseline fails to scale beyond two SSDs due to interconnect bottlenecks. With 16 \times CSDs, INF² reaches a 3.71 \times speedup, with additional cost 16 \times \$2,400. Notably, cost-efficiency of INF² gradually improves as more

CSDs are added, a significant advantage when considering scalability.

Against upgrading GPUs. As shown in Figure 17, upgrading from the A100 (\$7,000) to the H100 (\$30,000) only provides an 8%-19% throughput improvement with the baseline, as the main bottleneck remains KV cache-related I/O. In contrast, INF² reduces the system interconnect bottleneck, providing a 1.21×-1.69× speedup by replacing 8 storage devices with 8×CSDs (from \$400 to \$2,000 each). Replacing all storage devices with 16×CSDs results in a 2.15×-2.19× speedup, further improving cost efficiency compared to 8×CSDs. The only exception is the 30B model, where 8×CSDs achieve better cost efficiency due to X-cache, which effectively utilizes host memory space. Therefore, INF² provides much higher improvements per dollar than upgrading the GPU with offloading-based batched inference.

Against multi-GPU systems. We compared the cost-effectiveness of INF² with GPU-only solutions based on values reported in [99]. In SmoothQuant [99] (Tab.7), the per-token decoding latency for 1K context length with 175B model in FP16 with a batch size of 16 is 4133 ms, which can be converted to throughput of 3.88 token/sec. This setup uses 8×A100 80GB GPUs, with a system cost of \$199,000. In contrast, INF² achieves 1.99 token/sec for 175B 1K context lengths, as shown in Figure 15(a), at a total cost of \$98,400 (H100: \$30,000, server: \$20,000, expansion: \$10,000, and 16×CSD: \$38,400). We achieve better cost efficiency, with the GPU solution delivering 1.95e-5 throughput/\$ and INF² delivering 2.02e-5 throughput/\$.

8 Discussion

Storage Expansion and Resource Pooling. Modern workloads, such as LLMs [44], recommendation systems [92, 111], and big data analytics [33, 74], demand increasing memory and storage capacity. This has led to new approaches where multiple servers share storage and memory resources [22, 31]. INF² also leverages a storage expansion system [19, 44, 74, 92] with PCIe switches to accommodate multiple CSDs, aligning with this trend toward resource sharing.

However, the primary limitation of this solution lies in the host. Even with peer-to-peer communication [104], managing and scheduling data transfers place a heavy burden on the host [97]. Some works propose accelerator-orchestrated storage access [19, 74, 97], and INF² could benefit from such techniques. INF² also benefits from reduction of CPU burden through X-cache during LLM inference.

Another limitation of expansion systems is that they don't increase the physical slots or bandwidth available to the host, worsening the link bandwidth bottleneck as more devices are added. Smart-Infinity [44], which also utilizes CSDs, addresses this by increasing internal bandwidth in LLM training scenarios. While Smart-Infinity focuses on training, INF² is designed specifically for LLM inference.

9 Related Work

9.1 LLM Inference

LLM Inference Acceleration. Recent works have proposed various ways to accelerate LLM inference. These works either employed kernel optimizations [12, 98], offload memory-bound computation to PIM processors [40, 57, 69, 110], quantized parameters [26, 42, 63, 108], exploit model parallelism [12, 70], or devise new batching strategies [6, 23, 101]. These proposed methods have significantly improved the throughput of LLM inference systems, but they focus on interactive use cases. LLMs are also actively applied to offline scenarios, such as benchmarking [34, 35, 58, 109] and information extraction [20, 32, 67, 68, 71]. We target scenarios that are less sensitive to latency factors in batches over a large number of tokens running LLM inference.

Offloaded LLM Inference. As model sizes of recent LLMs grew exponentially, efficiently deploying these models on limited GPU resources became of crucial importance. Numerous studies on model training have addressed this issue by offloading data and computation to neighboring devices [14, 44, 76, 77]. Therefore, it was a natural next step to apply similar techniques for model inference. As a result, recent works offloaded data to storage systems [8, 45, 84] and also offloaded computation to the host CPU [84, 89, 107]. Similar to INF², these works offload computation from the GPU in order to alleviate the computational burdens of the GPU and reduce data movement between the devices. However, INF² is able to utilize much higher bandwidth compared to other works by employing CSDs.

9.2 Near-Data Processing

Processing In Memory. In the late 2010s, Processing In Memory (PIM) designs supporting more general computations started to appear [38, 52, 53], and real-world PIM products were introduced [27, 52, 53]. As these designs enabled more general computations, some works attempted to accelerate end-to-end LLM inference systems [57, 110]. Other works [40, 69] have explored PIM systems accompanied by GPUs or NPUs, where only selected memory-bound operations are offloaded to PIM processors. Although these works successfully increase throughput by offloading memory-bound applications to PIM, they are limited in that they have been evaluated in simulated environments only.

Near-Storage Processing. Various works explored ways to enable near-storage processing. Earlier works aimed to design "active" or "intelligent" disks [4, 48, 78, 79]. However, due to the massive advancements in the computing capabilities of existing processors, the idea of on-disk processing slowly faded away. Multiple studies proposed to accelerate various applications by either processing data utilizing the embedded CPU [47, 73] or integrating processors to each internal channel [13, 33] to exploit the internal bandwidth. Despite the effort, the embedded cores turned

out to be low in computational power. This led to utilizing dedicated processors for SSDs, such as ASICs [60, 64, 65] or FPGAs [86, 91, 96, 100]. These computational SSD products are available on the market [87] and are being used to accelerate various applications such as query processing [29], training deep learning models [44, 55], and deep learning model inference [88].

10 Conclusion

We propose INF², a novel framework for fast LLM inference using CSDs, achieving high throughput. By offloading KV-related operations to each CSD (attention-near storage), we significantly reduce the I/O overhead from KV caches. On top of attention-near storage, we introduce an efficient method for updating KV caches in storage that hides storage write latency (delayed KV cache writeback). Moreover, we fully leverage the new opportunities provided by CSDs. By storing input activations (X-cache) instead of K and V, we enable parallel computation between the GPU and CSDs with a limited main memory budget. INF² achieves up to 3.46× throughput improvement compared to state-of-the-art baselines. We will open-source INF² to encourage adoption and facilitate its use.

References

- [1] "Github Copilot." [Online]. Available: <https://github.com/features/copilot/>
- [2] "mdadm." [Online]. Available: <https://git.kernel.org/pub/scm/utils/mdadm/mdadm.git/>
- [3] "Xilinx OpenCL extension." [Online]. Available: https://xilinx.github.io/XRT/master/html/opencl_extension.html
- [4] A. Acharya, M. Uysal, and J. Saltz, "Active disks: programming model, algorithms and evaluation," in *ASPLOS*, 1998.
- [5] J. Achiam, S. Adler, S. Agarwal, L. Ahmad, I. Akkaya, F. L. Aleman, D. Almeida, J. Altschmidt, S. Altman, S. Anadkat *et al.*, "Gpt-4 technical report," *arXiv preprint arXiv:2303.08774*, 2023.
- [6] A. Agrawal, A. Panwar, J. Mohan, N. Kwatra, B. S. Gulavani, and R. Ramjee, "Sarathi: Efficient llm inference by piggybacking decodes with chunked prefills," *arXiv preprint arXiv:2308.16369*, 2023.
- [7] J. Ainslie, J. Lee-Thorp, M. de Jong, Y. Zemlyanskiy, F. Lebrón, and S. Sanghai, "GQA: Training Generalized Multi-query Transformer Models from Multi-head Checkpoints," *arXiv preprint arXiv:2305.13245*, 2023.
- [8] K. Alizadeh, I. Mirzadeh, D. Belenko, K. Khatamifard, M. Cho, C. C. Del Mundo, M. Rastegari, and M. Farajtabar, "Llm in a flash: Efficient large language model inference with limited memory," *arXiv preprint arXiv:2312.11514*, 2023.
- [9] T. Allen and R. Ge, "In-depth Analyses of Unified Virtual Memory System for GPU Accelerated Computing," in *SC*, 2021.
- [10] "AMD Kintex™ UltraScale+™ FPGAs." [Online]. Available: <https://www.amd.com/en/products/adaptive-socs-and-fpgas/fpga/kintex-ultrascale-plus.html>
- [11] AMD/Xilinx, "Vitis high-level synthesis user guide (ug1399)," 2021.
- [12] R. Y. Aminabadi, S. Rajbhandari, A. A. Awan, C. Li, D. Li, E. Zheng, O. Ruwase, S. Smith, M. Zhang, J. Rasley *et al.*, "Deepspeed-inference: enabling efficient inference of transformer models at unprecedented scale," in *SC*, 2022.
- [13] D.-H. Bae, J.-H. Kim, S.-W. Kim, H. Oh, and C. Park, "Intelligent SSD: a turbo for big data mining," in *CIKM*, 2013.
- [14] J. Bae, J. Lee, Y. Jin, S. Son, S. Kim, H. Jang, T. J. Ham, and J. W. Lee, "FlashNeuron: SSD-Enabled Large-Batch training of very deep neural networks," in *FAST*, 2021.
- [15] I. Beltagy, M. E. Peters, and A. Cohan, "Longformer: The long-document transformer," *arXiv preprint arXiv:2004.05150*, 2020.
- [16] S. Bergman, T. Brokhman, T. Cohen, and M. Silberstein, "SPIN: Seamless operating system integration of peer-to-peer DMA between SSDs and GPUs," *ACM Trans. Comput. Syst.*, vol. 36, no. 2, 2019.
- [17] A. Borzunov, D. Baranchuk, T. Dettmers, M. Ryabinin, Y. Belkada, A. Chumachenko, P. Samygin, and C. Raffel, "Petals: Collaborative inference and fine-tuning of large models," *arXiv preprint arXiv:2209.01188*, 2022.
- [18] T. Brown, B. Mann, N. Ryder, M. Subbiah, J. D. Kaplan, P. Dhariwal, A. Neelakantan, P. Shyam, G. Sastry, A. Askell, S. Agarwal, A. Herbert-Voss, G. Krueger, T. Henighan, R. Child, A. Ramesh, D. Ziegler, J. Wu, C. Winter, C. Hesse, M. Chen, E. Sigler, M. Litwin, S. Gray, B. Chess, J. Clark, C. Berner, S. McCandlish, A. Radford, I. Sutskever, and D. Amodei, "Language Models are Few-Shot Learners," in *NeurIPS*, 2020.
- [19] C.-H. Chang, J. Han, A. Sivasubramaniam, V. Sharma Mailthody, Z. Qureshi, and W.-M. Hwu, "GMT: GPU Orchestrated Memory Tiering for the Big Data Era," in *ASPLOS*, 2024.
- [20] Y. Chang, K. Lo, T. Goyal, and M. Iyyer, "BooookScore: A systematic exploration of book-length summarization in the era of LLMs," in *ICLR*, 2024.
- [21] Y. Chen, H. Xie, M. Ma, Y. Kang, X. Gao, L. Shi, Y. Cao, X. Gao, H. Fan, M. Wen, J. Zeng, S. Ghosh, X. Zhang, C. Zhang, Q. Lin, S. Rajmohan, D. Zhang, and T. Xu, "Automatic Root Cause Analysis via Large Language Models for Cloud Incidents," in *EuroSys*, 2024.
- [22] C. Consortium, "Compute express link." [Online]. Available: <https://www.computeexpresslink.org>
- [23] W. Cui, H. Zhao, Q. Chen, H. Wei, Z. Li, D. Zeng, C. Li, and M. Guo, "DVABatch: Diversity-aware Multi-Entry Multi-Exit Batching for Efficient Processing of DNN Services on GPUs," in *USENIX ATC*, 2022.
- [24] T. Dao, "FlashAttention-2: Faster Attention with Better Parallelism and Work Partitioning," in *ICLR*, 2024.
- [25] T. Dao, D. Fu, S. Ermon, A. Rudra, and C. Ré, "FlashAttention: Fast and Memory-Efficient Exact Attention with IO-Awareness," in *NeurIPS*, S. Koyejo, S. Mohamed, A. Agarwal, D. Belgrave, K. Cho, and A. Oh, Eds., 2022.
- [26] T. Dettmers, M. Lewis, Y. Belkada, and L. Zettlemoyer, "Gpt3. int8 (): 8-bit matrix multiplication for transformers at scale," in *NeurIPS*, 2022.
- [27] F. Devaux, "The true Processing In Memory accelerator," in *HCS*, 2019.
- [28] "Distutils." [Online]. Available: <https://docs.python.org/3.9/library/distutils.html>
- [29] J. Do, Y.-S. Kee, J. M. Patel, C. Park, K. Park, and D. J. DeWitt, "Query processing on smart SSDs: opportunities and challenges," in *SIGMOD*, 2013.
- [30] S. Elfving, E. Uchibe, and K. Doya, "Sigmoid-Weighted Linear Units for Neural Network Function Approximation in Reinforcement Learning," *Neural Networks*, vol. 107, pp. 3–11, 2018.
- [31] "Falcon 4109." [Online]. Available: <https://www.h3platform.com/product-detail/overview/25>
- [32] T. Goyal, J. J. Li, and G. Durrett, "News summarization and evaluation in the era of gpt-3," *arXiv preprint arXiv:2209.12356*, 2022.
- [33] B. Gu, A. S. Yoon, D.-H. Bae, I. Jo, J. Lee, J. Yoon, J.-U. Kang, M. Kwon, C. Yoon, S. Cho, J. Jeong, and D. Chang, "Biscuit: a framework for near-data processing of big data workloads," in *ISCA*, 2016.
- [34] N. Guha, J. Nyarko, D. Ho, C. Ré, A. Chilton, A. K. A. Chohlas-Wood, A. Peters, B. Waldon, D. Rockmore, D. Zambrano, D. Talisman,

- E. Hoque, F. Surani, F. Fagan, G. Sarfaty, G. Dickinson, H. Porat, J. Hegland, J. Wu, J. Nudell, J. Niklaus, J. Nay, J. Choi, K. Tobia, M. Hagan, M. Ma, M. Livermore, N. Rasumov-Rahe, N. Holzenberger, N. Kolt, P. Henderson, S. Rehaag, S. Goel, S. Gao, S. Williams, S. Gandhi, T. Zur, V. Iyer, and Z. Li, "LegalBench: A Collaboratively Built Benchmark for Measuring Legal Reasoning in Large Language Models," in *NeurIPS*, 2023.
- [35] J. Guo, L. Du, and H. Liu, "Gpt4graph: Can large language models understand graph structured data? an empirical evaluation and benchmarking," *arXiv preprint arXiv:2305.15066*, 2023.
- [36] L. Guo, Y. Chi, J. Lau, L. Song, X. Tian, M. Khatti, W. Qiao, J. Wang, E. Ustun, Z. Fang, Z. Zhang, and J. Cong, "TAPA: A Scalable Task-parallel Dataflow Programming Framework for Modern FPGAs with Co-optimization of HLS and Physical Design," *ACM TRETS*, vol. 16, no. 4, 2023.
- [37] L. Guo, Y. Chi, J. Wang, J. Lau, W. Qiao, E. Ustun, Z. Zhang, and J. Cong, "AutoBridge: Coupling Coarse-Grained Floorplanning and Pipelining for High-Frequency HLS Design on Multi-Die FPGAs," in *FPGA*, 2021, p. 81–92.
- [38] M. He, C. Song, I. Kim, C. Jeong, S. Kim, I. Park, M. Thottethodi, and T. N. Vijaykumar, "Newton: A DRAM-maker's Accelerator-in-Memory (AiM) Architecture for Machine Learning," in *MICRO*, 2020.
- [39] D. Hendrycks and K. Gimpel, "Gaussian error linear units (gelus)," *arXiv preprint arXiv:1606.08415*, 2016.
- [40] G. Heo, S. Lee, J. Cho, H. Choi, S. Lee, H. Ham, G. Kim, D. Mahajan, and J. Park, "NeuPIMs: NPU-PIM Heterogeneous Acceleration for Batched LLM Inferencing," in *ASPLOS*, 2024.
- [41] C. Holmes, M. Tanaka, M. Wyatt, A. A. Awan, J. Rasley, S. Rajbhandari, R. Y. Aminabadi, H. Qin, A. Bakhtiari, L. Kurilenko *et al.*, "DeepSpeed-Fastgen: High-throughput Text Generation for LLMs via MII and DeepSpeed-Inference," *arXiv preprint arXiv:2401.08671*, 2024.
- [42] C. Hooper, S. Kim, H. Mohammadzadeh, M. W. Mahoney, Y. S. Shao, K. Keutzer, and A. Gholami, "KVQuant: Towards 10 Million Context Length LLM Inference with KV Cache Quantization," *arXiv preprint arXiv:2401.18079*, 2024.
- [43] "Hugging Face." [Online]. Available: <https://huggingface.co/docs/hub/index>
- [44] H. Jang, J. Song, J. Jung, J. Park, Y. Kim, and J. Lee, "Smart-Infinity: Fast Large Language Model Training using Near-Storage Processing on a Real System," in *HPCA*, 2024.
- [45] Y. Jin, S. Kim, T. J. Ham, and J. W. Lee, "Architecting a Flash-Based Storage System for Low-Cost Inference of Extreme-Scale DNNs," *IEEE Transactions on Computers*, 2022.
- [46] H. Kang, Q. Zhang, S. Kundu, G. Jeong, Z. Liu, T. Krishna, and T. Zhao, "Gear: An efficient kv cache compression recipe for near-lossless generative inference of llm," *arXiv preprint arXiv:2403.05527*, 2024.
- [47] Y. Kang, Y.-s. Kee, E. L. Miller, and C. Park, "Enabling cost-effective data processing with smart SSD," in *MSST*, 2013.
- [48] K. Keeton, D. A. Patterson, and J. M. Hellerstein, "A case for intelligent disks (IDISKs)," *SIGMOD Rec.*, vol. 27, no. 3, 1998.
- [49] J. H. Kim, S.-h. Kang, S. Lee, H. Kim, W. Song, Y. Ro, S. Lee, D. Wang, H. Shin, B. Phuah, J. Choi, J. So, Y. Cho, J. Song, J. Choi, J. Cho, K. Sohn, Y. Sohn, K. Park, and N. S. Kim, "Aquabolt-xl: Samsung hbm2-pim with in-memory processing for ml accelerators and beyond," in *2021 IEEE Hot Chips 33 Symposium (HCS)*, 2021, pp. 1–26.
- [50] M. Kwon, D. Gouk, S. Lee, and M. Jung, "Hardware/Software Co-Programmable Framework for Computational SSDs to Accelerate Deep Learning Service on Large-Scale Graphs," in *FAST*, 2022.
- [51] W. Kwon, Z. Li, S. Zhuang, Y. Sheng, L. Zheng, C. H. Yu, J. Gonzalez, H. Zhang, and I. Stoica, "Efficient Memory Management for Large Language Model Serving with PagedAttention," in *SOSP*, 2023.
- [52] S. Lee, K. Kim, S. Oh, J. Park, G. Hong, D. Ka, K. Hwang, J. Park, K. Kang, J. Kim *et al.*, "A 1ynm 1.25 V 8Gb, 16Gb/s/pin GDDR6-based accelerator-in-memory supporting 1TFLOPS MAC operation and various activation functions for deep-learning applications," in *ISSCC*, 2022.
- [53] S. Lee, S.-h. Kang, J. Lee, H. Kim, E. Lee, S. Seo, H. Yoon, S. Lee, K. Lim, H. Shin, J. Kim, O. Seongil, A. Iyer, D. Wang, K. Sohn, and N. S. Kim, "Hardware Architecture and Software Stack for PIM Based on Commercial DRAM Technology : Industrial Product," in *ISCA*, 2021.
- [54] W. Lee, J. Lee, J. Seo, and J. Sim, "InfiniGen: Efficient Generative Inference of Large Language Models with Dynamic KV Cache Management," in *OSDI*, 2024.
- [55] Y. Lee, J. Chung, and M. Rhu, "SmartSAGE: training large-scale graph neural networks using in-storage processing architectures," in *ISCA*, 2022.
- [56] C. Li, Y. Wang, C. Liu, S. Liang, H. Li, and X. Li, "GLIST: Towards In-Storage Graph Learning," in *USENIX ATC*, 2021.
- [57] C. Li, Z. Zhou, Y. Wang, F. Yang, T. Cao, M. Yang, Y. Liang, and G. Sun, "PIM-DL: Expanding the Applicability of Commodity DRAM-PIMs for Deep Learning via Algorithm-System Co-Optimization," in *ASPLOS*, 2024.
- [58] P. Liang, R. Bommasani, T. Lee, D. Tsipras, D. Soylu, M. Yasunaga, Y. Zhang, D. Narayanan, Y. Wu, A. Kumar, B. Newman, B. Yuan, B. Yan, C. Zhang, C. A. Cosgrove, C. D. Manning, C. Re, D. Acosta-Navas, D. A. Hudson, E. Zelikman, E. Durmus, F. Ladhak, F. Rong, H. Ren, H. Yao, J. WANG, K. Santhanam, L. Orr, L. Zheng, M. Yuksekgonul, M. Suzgun, N. Kim, N. Guha, N. S. Chatterji, O. Khattab, P. Henderson, Q. Huang, R. A. Chi, S. M. Xie, S. Santurkar, S. Ganguli, T. Hashimoto, T. Icard, T. Zhang, V. Chaudhary, W. Wang, X. Li, Y. Mai, Y. Zhang, and Y. Koreeda, "Holistic Evaluation of Language Models," *Transactions on Machine Learning Research*, 2023.
- [59] B. Lin, T. Peng, C. Zhang, M. Sun, L. Li, H. Zhao, W. Xiao, Q. Xu, X. Qiu, S. Li *et al.*, "Infinite-LLM: Efficient LLM Service for Long Context with DistAttention and Distributed KVCache," *arXiv preprint arXiv:2401.02669*, 2024.
- [60] J. Lin, L. Liang, Z. Qu, I. Ahmad, L. Liu, F. Tu, T. Gupta, Y. Ding, and Y. Xie, "INSPIRE: In-Storage Private Information Retrieval via Protocol and Architecture Co-Design," in *ISCA*, 2022.
- [61] H. Liu and P. Abbeel, "Blockwise Parallel Transformers for Large Context Models," in *NeurIPS*, 2023.
- [62] H. Liu, M. Zaharia, and P. Abbeel, "Ring Attention with Blockwise Transformers for Near-infinite Context," *arXiv preprint arXiv:2310.01889*, 2023.
- [63] Z. Liu, B. Oguz, C. Zhao, E. Chang, P. Stock, Y. Mehdad, Y. Shi, R. Krishnamoorthi, and V. Chandra, "Llm-qat: Data-free quantization aware training for large language models," *arXiv preprint arXiv:2305.17888*, 2023.
- [64] V. S. Mailthody, Z. Qureshi, W. Liang, Z. Feng, S. G. De Gonzalo, Y. Li, H. Franke, J. Xiong, J. Huang, and W.-m. Hwu, "Deepstore: In-storage acceleration for intelligent queries," in *MICRO*, 2019.
- [65] N. Mansouri Ghiasi, J. Park, H. Mustafa, J. Kim, A. Olgun, A. Gollwitzer, D. Senol Cali, C. Firtina, H. Mao, N. Almadhoun Alser, R. Ausavarungnirun, N. Vijaykumar, M. Alser, and O. Mutlu, "GenStore: a high-performance in-storage processing system for genome sequence analysis," in *ASPLOS*, 2022.
- [66] C. Mead and L. Conway, "Introduction to VLSI systems," 1980.
- [67] S. Narayan, S. B. Cohen, and M. Lapata, "Don't give me the details, just the summary! topic-aware convolutional neural networks for extreme summarization," *arXiv preprint arXiv:1808.08745*, 2018.
- [68] B. Pang, E. Nijkamp, W. Kryscinski, S. Savarese, Y. Zhou, and C. Xiong, "Long Document Summarization with Top-down and Bottom-up Inference," in *EACL*, 2023.
- [69] J. Park, J. Choi, K. Kyung, M. J. Kim, Y. Kwon, N. S. Kim, and J. H. Ahn, "AttAcc! Unleashing the Power of PIM for Batched Transformer-based Generative Model Inference," in *ASPLOS*, 2024.

- [70] R. Pope, S. Douglas, A. Chowdhery, J. Devlin, J. Bradbury, J. Heek, K. Xiao, S. Agrawal, and J. Dean, "Efficiently scaling transformer inference," in *MLSys*, 2023.
- [71] X. Pu, M. Gao, and X. Wan, "Summarization is (almost) dead," *arXiv preprint arXiv:2309.09558*, 2023.
- [72] "pybind11." [Online]. Available: <https://github.com/pybind/pybind11>
- [73] L. C. Quero, Y.-S. Lee, and J.-S. Kim, "Self-sorting SSD: Producing sorted data inside active SSDs," in *MSST*, 2015.
- [74] Z. Qureshi, V. S. Malthody, I. Gelado, S. Min, A. Masood, J. Park, J. Xiong, C. J. Newburn, D. Vainbrand, I.-H. Chung, M. Garland, W. Dally, and W.-m. Hwu, "GPU-Initiated On-Demand High-Throughput Storage Access in the BaM System Architecture," in *ASPLOS*, 2023.
- [75] A. Radford, J. Wu, R. Child, D. Luan, D. Amodei, and I. Sutskever, "Language Models Are Unsupervised Multitask Learners," *OpenAI blog*, 2019.
- [76] S. Rajbhandari, O. Ruwase, J. Rasley, S. Smith, and Y. He, "ZeRO-infinity: breaking the GPU memory wall for extreme scale deep learning," in *SC*, 2021.
- [77] J. Ren, S. Rajbhandari, R. Y. Aminabadi, O. Ruwase, S. Yang, M. Zhang, D. Li, and Y. He, "Zero-offload: democratizing billion-scale model training," in *USENIX ATC*, 2021.
- [78] E. Riedel, C. Faloutsos, G. Gibson, and D. Nagle, "Active disks for large-scale data processing," *Computer*, vol. 34, no. 6, pp. 68–74, 2001.
- [79] E. Riedel, G. A. Gibson, and C. Faloutsos, "Active Storage for Large-Scale Data Mining and Multimedia," in *VLDB*, 1998.
- [80] S. Salamat, A. Haj Aboutalebi, B. Khaleghi, J. H. Lee, Y. S. Ki, and T. Rosing, "NASCENT: Near-storage acceleration of database sort on SmartSSD," in *FPGA*, 2021.
- [81] S. Salamat, H. Zhang, Y. S. Ki, and T. Rosing, "NASCENT2: Generic near-storage sort accelerator for data analytics on SmartSSD," *ACM TRETS*, 2022.
- [82] R. Schmid, M. Plauth, L. Wenzel, F. Eberhardt, and A. Polze, "Accessible near-storage computing with FPGAs," in *EuroSys*, 2020.
- [83] Y. Seneviratne, K. Seemakhuft, S. Liu, and S. Khan, "NearPM: A Near-Data Processing System for Storage-Class Applications," in *EuroSys*, 2023.
- [84] Y. Sheng, L. Zheng, B. Yuan, Z. Li, M. Ryabinin, B. Chen, P. Liang, C. Re, I. Stoica, and C. Zhang, "FlexGen: High-Throughput Generative Inference of Large Language Models with a Single GPU," in *ICML*, 2023.
- [85] M. Shoeybi, M. Patwary, R. Puri, P. LeGresley, J. Casper, and B. Catanzaro, "Megatron-lm: Training multi-billion parameter language models using model parallelism," *arXiv preprint arXiv:1909.08053*, 2019.
- [86] M. Singh and B. Leonhardi, "Introduction to the IBM Netezza warehouse appliance," in *CASCON*, 2011.
- [87] "SmartSSD." [Online]. Available: <https://www.xilinx.com/applications/data-center/computational-storage/smartssd.html>
- [88] M. Soltaniyeh, V. Lagrange Moutinho Dos Reis, M. Bryson, X. Yao, R. P. Martin, and S. Nagarakatte, "Near-Storage Processing for Solid State Drive Based Recommendation Inference with SmartSSDs®," in *ICPE*, 2022.
- [89] Y. Song, Z. Mi, H. Xie, and H. Chen, "Powerinfer: Fast large language model serving with a consumer-grade gpu," *arXiv preprint arXiv:2312.12456*, 2023.
- [90] J. Sun, M. Sun, Z. Zhang, J. Xie, Z. Shi, Z. Yang, J. Zhang, F. Wu, and Z. Wang, "Helios: An Efficient Out-of-core GNN Training System on Terabyte-scale Graphs with In-memory Performance," *arXiv preprint arXiv:2310.00837*, 2023.
- [91] X. Sun, H. Wan, Q. Li, C.-L. Yang, T.-W. Kuo, and C. J. Xue, "RM-SSD: In-storage computing for large-scale recommendation inference," in *HPCA*, 2022.
- [92] B. Tian, H. Liu, Z. Duan, X. Liao, H. Jin, and Y. Zhang, "Scalable Billion-point Approximate Nearest Neighbor Search Using SmartSSDs," in *USENIX ATC*, 2024.
- [93] H. Touvron, T. Lavril, G. Izacard, X. Martinet, M.-A. Lachaux, T. Lacroix, B. Rozière, N. Goyal, E. Hambro, F. Azhar *et al.*, "Llama: Open and efficient foundation language models," *arXiv preprint arXiv:2302.13971*, 2023.
- [94] H. Touvron, L. Martin, K. Stone, P. Albert, A. Almahairi, Y. Babaei, N. Bashlykov, S. Batra, P. Bhargava, S. Bhosale *et al.*, "Llama 2: Open Foundation and Fine-tuned Chat Models," *arXiv preprint arXiv:2307.09288*, 2023.
- [95] A. Vaswani, N. Shazeer, N. Parmar, J. Uszkoreit, L. Jones, A. N. Gomez, L. u. Kaiser, and I. Polosukhin, "Attention is All You Need," in *NeurIPS*, 2017.
- [96] R. Weiss, "A technical overview of the oracle exadata database machine and exadata storage server," *Oracle White Paper*, 2012.
- [97] L. Y. Wong, J. Zhang, and J. J. Li, "DONGLE: Direct FPGA-orchestrated NVMe storage for HLS," in *FPGA*, 2023.
- [98] H. Xia, Z. Zheng, Y. Li, D. Zhuang, Z. Zhou, X. Qiu, Y. Li, W. Lin, and S. L. Song, "Flash-LLM: Enabling Cost-Effective and Highly-Efficient Large Generative Model Inference with Unstructured Sparsity," *Proc. VLDB Endow.*, 2023.
- [99] G. Xiao, J. Lin, M. Seznec, H. Wu, J. Demouth, and S. Han, "SmoothQuant: Accurate and Efficient Post-Training Quantization for Large Language Models," in *ICML*, 2023.
- [100] W. Xiong, L. Ke, D. Jankov, M. Kounavis, X. Wang, E. Northup, J. Yang, B. Acun, C. Wu, P. P. Tang, G. E. Suh, X. Zhang, and H. S. Lee, "SecNDP: Secure Near-Data Processing with Untrusted Memory," in *HPCA*, 2022.
- [101] G.-I. Yu, J. S. Jeong, G.-W. Kim, S. Kim, and B.-G. Chun, "Orca: A Distributed Serving System for Transformer-Based Generative Models," in *OSDI*, 2022.
- [102] M. Zaheer, G. Guruganesh, A. Dubey, J. Ainslie, C. Alberti, S. Ontanon, P. Pham, A. Ravula, Q. Wang, L. Yang, and A. Ahmed, "Big bird: transformers for longer sequences," in *NeurIPS*, 2020.
- [103] J. Zhang, Y. Ren, M. Nguyen, C. Min, and S. Kannan, "OmniCache: Collaborative Caching for Near-storage Accelerators," in *FAST*, 2024.
- [104] J. Zhang, D. Donofrio, J. Shalf, M. T. Kandemir, and M. Jung, "NVMMU: A non-volatile memory management unit for heterogeneous GPU-SSD architectures," in *PACT*, 2015.
- [105] S. Zhang, S. Roller, N. Goyal, M. Artetxe, M. Chen, S. Chen, C. Dewan, M. Diab, X. Li, X. V. Lin *et al.*, "Opt: Open pre-trained transformer language models," *arXiv preprint arXiv:2205.01068*, 2022.
- [106] Z. Zhang, Y. Sheng, T. Zhou, T. Chen, L. Zheng, R. Cai, Z. Song, Y. Tian, C. Ré, C. Barrett, Z. A. Wang, and B. Chen, "H2O: Heavy-Hitter Oracle for Efficient Generative Inference of Large Language Models," in *NeurIPS*, A. Oh, T. Naumann, A. Globerson, K. Saenko, M. Hardt, and S. Levine, Eds., 2023.
- [107] X. Zhao, B. Jia, H. Zhou, Z. Liu, S. Cheng, and Y. You, "HeteGen: Heterogeneous Parallel Inference for Large Language Models on Resource-Constrained Devices," *arXiv preprint arXiv:2403.01164*, 2024.
- [108] Y. Zhao, C.-Y. Lin, K. Zhu, Z. Ye, L. Chen, S. Zheng, L. Ceze, A. Krishnamurthy, T. Chen, and B. Kasikci, "Atom: Low-bit quantization for efficient and accurate llm serving," *arXiv preprint arXiv:2310.19102*, 2023.
- [109] L. Zheng, W.-L. Chiang, Y. Sheng, S. Zhuang, Z. Wu, Y. Zhuang, Z. Lin, Z. Li, D. Li, E. Xing, H. Zhang, J. E. Gonzalez, and I. Stoica, "Judging LLM-as-a-Judge with MT-Bench and Chatbot Arena," in *NeurIPS*, 2023.
- [110] M. Zhou, W. Xu, J. Kang, and T. Rosing, "TransPIM: A Memory-based Acceleration via Software-Hardware Co-Design for Transformer," in *HPCA*, 2022.
- [111] R. Zhou, S. Khemmarat, and L. Gao, "The impact of YouTube recommendation system on video views," in *SIGCOMM*, 2010.